

Structural and Chiroptical Properties of Acyclic and Macrocyclic 1,5-Bis(oxazoline) Ligands and Their Copper(I) and Silver(I) Complexes

Miklos Hollosi,^[a] Zsuzsa Majer,^[a] Elemér Vass,^[a] Zlata Raza,^[b] Vladislav Tomišić,^[c] Tomislav Portada,^[b] Ivo Piantanida,^[b] Mladen Žinić,^[b] and Vitomir Sunjić*^[b]

Keywords: Circular dichroism / Conformation analysis / Copper / Silver / Bis(oxazoline) ligands / Macrocyclic ligands

C₂-symmetric acyclic ligands **1a–1e**, macrocyclic ligands **2a–2d** and **3**, and their copper(I) and silver(I) complexes were studied by UV, NMR and CD spectroscopy. The stability constants of the metal–**1a** and –**1b** complexes with 1:1 and 1:2 stoichiometries in acetonitrile were determined by spectrometric titrations. Evidence of tetrahedral coordination for complex [Ag(**1a**)₂]⁺ was obtained from the complexation induced shifts (CIS) and NOEs, and corroborated by molecular modeling. Ligands with phenyl rings on the stereogenic cen-

ters (**1a,c** and **2**) exhibit a strong Cotton effect (CE) in the region of the ¹B_b band, which is absent in the ligands with benzyl groups on the stereogenic center (**1b, 3**). This effect is ascribed to the exciton coupling (EC) of two aromatic chromophores on the stereogenic center. For ligands **1a** and **2a** the EC changes the sign on complexation to Cu⁺, revealing opposite helicity of the free and complexed ligand. (© Wiley-VCH Verlag GmbH, 69451 Weinheim, Germany, 2002)

Introduction

Chiral bis(oxazoline)–metal complexes have received a great deal of attention through their use in various asymmetric catalytic processes.^[1–4] Among them the complexes with 1,5-bis(oxazoline) ligands having one carbon spacer between the oxazoline rings and able to form six-membered metal chelates, are the most frequently utilized as chiral catalytic complexes in various enantioselective transformations.

The most explored catalytic complexes are those of copper(I)^[5–14] (enantioselective cyclopropanation of alkenes,^[5–11] aziridation of olefins^[12] and imines,^[13] allylic oxidation of cycloalkenes^[14]), copper(II)^[15–24] (Diels–Alder reaction,^[15–19] Mukaiyama aldol reaction,^[20] Mukaiyama–Michael addition reaction,^[21,22] Friedel–Crafts reaction,^[23] Canizzaro reaction^[24]), palladium(II)^[25–27] (allylic substitution reaction), and zinc(II)^[28–30] (allylation reaction). We have recently reported on very high cumulative enantio- and diastereoselectivity in cyclopropanation of styrene catalyzed by copper(I) complexes of macrocyclic ligands **2a–2c** (Figure 1).^[31]

These results are in line with our previous observation,^[32,33] that enantioselectivity enhancement can be achieved by restricting conformational mobility of the ligand by repulsive or attractive π – π interactions.^[34–36]

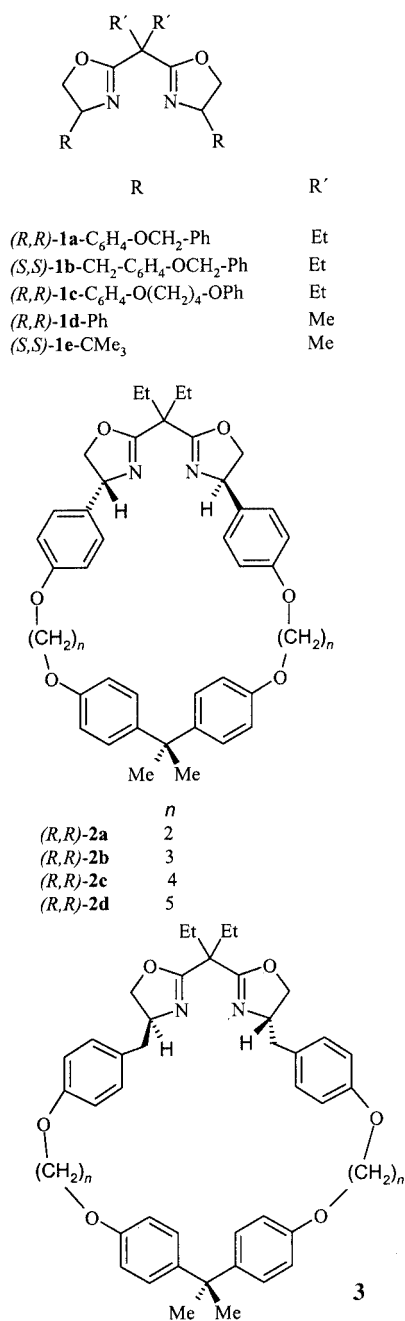
Structural studies of the ligand–metal complexes often provide valuable information regarding transition state assembly in the catalytic transformation. Already, the solid-state structures of various bis(oxazoline)–metal complexes have been elucidated on the basis of X-ray diffraction analysis,^[5,9,19,26,27,37–44] but only a few were determined in solution based on NMR^[26,38,43–45] and CD^[44,45] spectroscopic investigations. To the best of our knowledge, the spectroscopic study of 1,5-bis(oxazoline)–copper(I) and –silver(I) complexes in solution, aimed at elucidating their structure and stability, has not been performed to date. Herewith we report the results of the combined achiral (UV, fluorimetric, ES-MS, NMR) and chiroptical (CD) spectroscopic studies of the acyclic (**1**) and macrocyclic ligands (**2, 3**) (Figure 1) as well as their Cu⁺ and Ag⁺ complexes, corroborated by molecular modeling of some selected complexes. The study was expected to give insight into the topology of the free ligands and complexes, identify the stoichiometry, stability and structure of the complexes, and consequently to shed more light on the origin of stereoselectivity exhibited by this type of bisoxazoline ligands.

After this study was completed, a paper of Walsh et al.^[46] appeared reporting on the study of the conformation of flexible macrocyclic catalysts in solution. The results support that bis(sulfonamido) ligands, derived from (*R,R*)-1,2-

^[a] Eötvös Loránd University, Department of Organic Chemistry P. O. Box 32, 1518 Budapest, Hungary

^[b] Department of Organic Chemistry and Biochemistry, “Rudjer Bošković” Institute, P. O. Box 180, 10002 Zagreb, Croatia Fax: (internat.) + 385-1/468-0195 E-mail: sunjic@rudjer.irb.hr

^[c] Laboratory of Physical Chemistry, Faculty of Science, University of Zagreb, P. O. Box 163, 10001 Zagreb, Croatia

Figure 1. Formulae **1**–**3**

diaminocyclohexane, are bound to the catalytic metal ion in a C_2 -symmetric conformation in the transition state of the asymmetric addition of Et₂Zn to benzaldehyde.

Results and Discussion

Spectrometric Studies of Copper(I) and Silver(I) Complexes of **1a** and **1b**

The copper(I) and silver(I) complexing properties of ligands **1a** and **1b** have been investigated by spectrometric (UV, NMR, and fluorimetric) titrations. The obtained spectrometric data were processed using the SPECFIT pro-

gram.^[47] The addition of Cu⁺ into the MeCN solutions of both **1a** and **1b** caused a hyperchromic effect in the corresponding UV spectra (Figure 2). Among several chemically reasonable speciations used in the fitting of the spectrophotometric data, two (set by assuming the presence of [CuL]⁺ and [CuL₂]⁺ or [CuL₂]⁺ and [Cu₂L₂]²⁺; L standing for either **1a** or **1b**) gave satisfactory results. However, the electrospray mass spectrometry (ES-MS) experiments indicated formation of [CuL]⁺ and [CuL₂]⁺ complexes and no evidence of the presence of [Cu₂L₂]²⁺ species was observed. The mass spectra of MeCN solutions of Cu⁺/**1a** with various $c(\text{Cu}^+)/c(\textbf{1a})$ ratios showed peaks at $m/z = 678$ {[Cu(**1a**)(MeCN)]_{*n*}⁺} and 1212 {[Cu(**1a**)₂]⁺}, while in the case of Cu⁺/**1b** peaks were observed at 665 {[Cu(**1b**)]_{*n*}⁺} and 1268 {[Cu(**1b**)₂]⁺}, a very weak signal, presumably due to the fragmentation in the mass spectrometer. The isotopic abundances of the peaks at $m/z = 678$ and 665 showed peak separation of 1 Da, supporting the presence of singly charged species, i.e. [CuL]⁺. The stability constants of the Cu⁺ complexes calculated from the spectrophotometric titration data are collected in Table 1. Both, **1a** and **1b** form quite stable 1:1 ($K_{\text{CuL}} \approx 10^5 \text{ M}^{-1}$) and 1:2 ($K_{\text{CuL}_2} \approx 10^4 \text{ M}^{-1}$) complexes with Cu⁺ in MeCN.

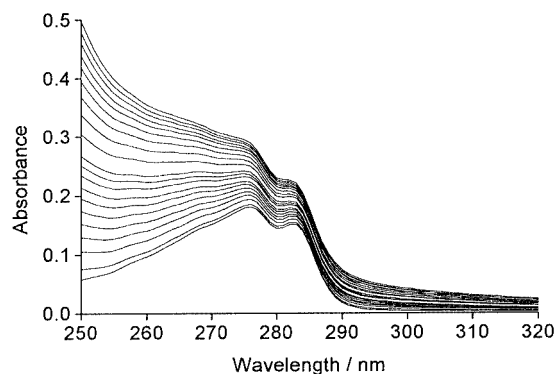


Figure 2. Spectrophotometric titration of **1a** ($c = 5 \cdot 10^{-5} \text{ mol} \cdot \text{dm}^{-3}$) with [(CH₃CN)₄Cu]PF₆ in MeCN; $l = 1 \text{ cm}$; $\varphi = 25^\circ \text{C}$; $c(\text{Cu}^+) = 0$ (bottom curve) to $1.7 \cdot 10^{-4} \text{ mol} \cdot \text{dm}^{-3}$ (top curve); the spectra are corrected for dilution

Table 1. Stability constants of Cu⁺ and Ag⁺ complexes with **1a** and **1b** in MeCN determined by UV, ¹H NMR, and fluorimetric titrations; numbers in parentheses are estimated errors of the last digit

Species	log $K^{[a]}$		
	UV	¹ H NMR	Fluorimetry
Cu(1a)	5.23(5)		
Cu(1a) ₂	4.2(2)		
Cu(1b)	5.07(3)		
Cu(1b) ₂	4.2(1)		
Ag(1a)		3.49(7)	3.45(6)
Ag(1a) ₂		3.27(8)	
Ag(1b)		3.92(7)	3.63(4)
Ag(1b) ₂		3.1(2)	

^[a] $K = [\text{ML}_n]/([\text{ML}_{n-1}][\text{L}])$; M standing for Cu⁺ or Ag⁺ and L for **1a** or **1b**; $n = 1, 2$.

The UV spectral changes recorded during the titrations of **1a** and **1b** with Ag^+ in MeCN had qualitatively the same trend as in the case of Cu^+ , but were insufficient to enable accurate analysis. Therefore, the formation of Ag^+ complexes was studied by means of ^1H NMR and fluorimetric titrations. The ^1H NMR spectra of **1a** and **1b** in $[\text{D}_3]\text{MeCN}$ are concentration-independent in the range of $2 \cdot 10^{-3}$ to $2 \cdot 10^{-2} \text{ mol} \cdot \text{dm}^{-3}$. The addition of AgBF_4 to **1a** up to the ratio $c(\text{Ag}^+)/c(\text{1a}) = 0.5$ induced shielding of all protons except that of $\text{C}(5)\text{--H}_{\text{trans}}$ (Figures 3 and 4, a). Further addition [$c(\text{Ag}^+)/c(\text{1a}) = 0.5\text{--}2.0$] resulted in a deshielding effect. The shielding/deshielding effect changed at the ratio $c(\text{Ag}^+)/c(\text{1a}) = 0.5$ indicating the initial formation of $[\text{Ag}(\text{1a})_2]^+$ species. Accordingly, the titration data were best fitted with a model including $[\text{Ag}(\text{1a})]^+$ and $[\text{Ag}(\text{1a})_2]^+$ complexes. The addition of Ag^+ to the solution of **1b** caused deshielding of all proton signals except for those of the methyl groups, which were shielded. However, the data were again best fitted with the model including two complex species, $[\text{Ag}(\text{1b})]^+$ and $[\text{Ag}(\text{1b})_2]^+$. Comparison of the determined stability constants of Ag^+ complexes with those of Cu^+ complexes (Table 1) shows that the former are more than one order of magnitude less stable for both ligands **1a** and **1b**.

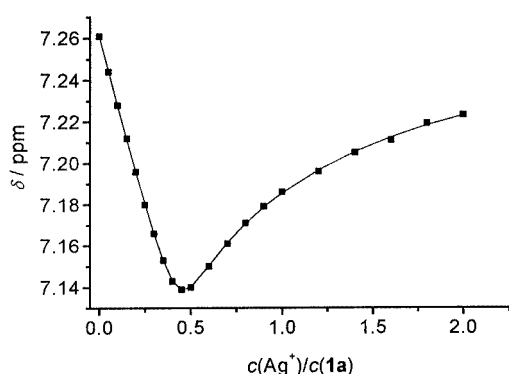


Figure 3. Experimental (dots) and calculated (line) chemical shifts of $\text{C}(2')\text{--H}$ of **1a** induced by addition of AgBF_4 (solvent: $[\text{D}_3]\text{MeCN}$)

The stabilities of the **1a**– and **1b**– Ag^+ complexes were also determined by means of fluorimetry. In MeCN ligands **1a** and **1b** exhibited a concentration-independent fluorescence up to the concentration of $2 \cdot 10^{-5} \text{ mol} \cdot \text{dm}^{-3}$. The addition of Ag^+ quenched the fluorescence of **1a** and **1b** for ca. 90%. Processing of the titration data gave good fits when only the $[\text{AgL}]^+$ complex formation was taken into account for both compounds. The absence of $[\text{AgL}_2]^+$ could be explained assuming that fluorimetric properties of this species are similar to those of the free ligand causing insignificant spectral changes. On the other hand, the $[\text{AgL}]^+$ complexes exhibit a much weaker emission than free **1a** and **1b**. Consequently, titration data were collected mostly under conditions preferable for 1:1 stoichiometry and only the formation of $[\text{Ag}(\text{1a})]^+$ and $[\text{Ag}(\text{1b})]^+$ was observed. As can be seen in Table 1, the stability constants of these complexes determined by fluorimetric and ^1H NMR titrations are in

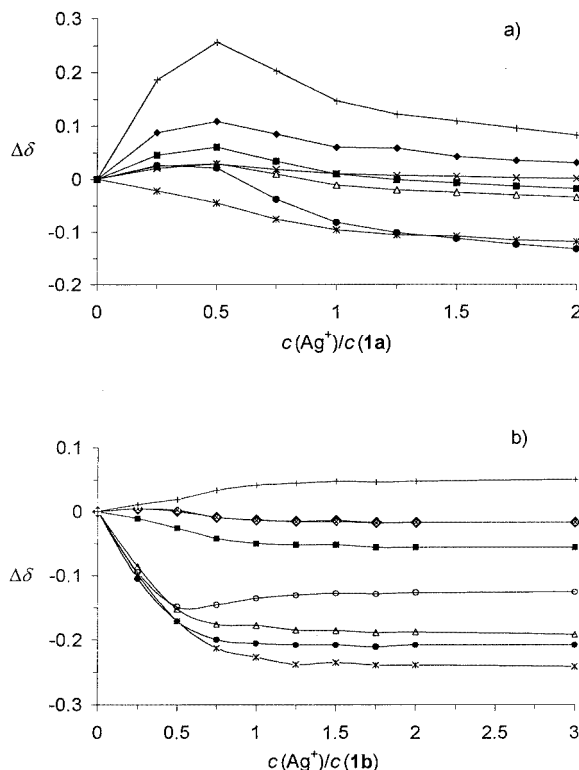


Figure 4. Complexation-induced shifts for **1a**– and **1b**– Ag^+ complexes; a): (+) CH_3 ; (◆) $\text{C}(2')\text{--H}$; (×) $\text{C}(4')\text{--OCH}_2$; (■) $\text{C}(3')\text{--H}$; (Δ) $\text{C}(4)\text{--H}$; (*) $\text{C}(5)\text{--H}_{\text{trans}}$; (●) $\text{C}(5)\text{--H}_{\text{cis}}$; b): (O) $\text{C}(4)\text{--CH}_2$

rather good agreement. The stoichiometries of the Ag^+ complexes were additionally confirmed by electrospray mass spectrometry which showed peaks at $m/z = 683$ $\{[\text{Ag}(\text{1a})]_n^{n+}\}$, 1258 $\{[\text{Ag}(\text{1a})_2]^+\}$ and 711 $\{[\text{Ag}(\text{1b})]_n^{n+}\}$. The exception was the absence of the signals of the $[\text{Ag}(\text{1b})_2]^+$ species that could be attributed to the fragmentation in the mass spectrometer and to the equilibrium in solution (see next paragraph and Figure 6). The isotopic abundances of the peaks at $m/z = 683$ and 711 showed peak separation of 1 Da, corresponding to the singly charged species $[\text{Ag}(\text{1a})]^+$ and $[\text{Ag}(\text{1b})]^+$, respectively.

Complexation-Induced Shifts (CIS) and NOEs in the ^1H NMR Spectra of the $\text{Ag}\text{--}1\text{a,b}$ Complexes

Structure of Complex $[\text{Ag}(\text{1a})_2]^+$

Addition of Ag^+ to **1a** produced significant shifts of all the resonances of **1a**, without line broadening. This indicates fast equilibrium kinetics on the NMR time scale. The observed complexation induced shifts of **1a**, expressed as $\Delta\delta = \delta\text{H}_{\text{lig}} - \delta\text{H}_{\text{compl}}$ (ppm), were plotted against the $c(\text{Ag}^+)/c(\text{1a})$ ratio (Figure 4, a). Ag^+ was added until a ratio of 0.5 was reached for the induced upfield shifts of all **1a** resonances except that of $\text{C}(5)\text{--H}_{\text{trans}}$; further additions of the cation produced downfield shifts of all resonances. A clear maximum at a $c(\text{Ag}^+)/c(\text{1a})$ value of 0.5 suggests initial formation of the $\text{Ag}^+\text{--}1\text{a}$ complex in a 1:2 stoichiometry which at higher ratios transforms to the 1:1 com-

plex. The methyl groups at the bis(oxazoline) bridge as well as the aromatic C(2')–H and C(3')–H groups experience the strongest shielding effects in the $[\text{Ag}(\mathbf{1a})_2]^+$ complex, which strongly suggests formation of the tetrahedral Ag^+ complex with the cation bound to 4 nitrogen atoms of the two orthogonally oriented bis(oxazoline) units of the $\mathbf{1a}$ molecules. The molecular models (see next paragraph and Figure 7, a) shows that in such a complex each bis(oxazoline) unit is located between two phenyl groups of the second ligand molecule. The C(4)-phenyl groups of two ligands end up close to one another, which results in the shielding of C(2')–H and C(3')–H. The methyl groups and the C(4)–H and C(5)–H_{cis} atoms of each bis(oxazoline) unit are also shielded by C(4)-phenyl groups of the second ligand. Additional support for the occurrence of such a 1:2 complex comes from the analysis of the NOESY spectrum at a $c(\text{Ag}^+)/c(\mathbf{1a})$ ratio of 0.5. The observed NOE interactions are shown in Figure 5. The molecular model of $\mathbf{1a}$ shows that the majority of the observed NOE crosspeaks could be explained by the favorable distances between respective hydrogen atoms in a single $\mathbf{1a}$ molecule. However, a clear crosspeak corresponding to NOE interactions between C(4')–OCH₂ and methyl protons of the bis(oxazoline) bridge is observed. The closest possible distance between these protons in the model of $\mathbf{1a}$ is ca. 8 Å, well exceeding the limiting value of 4–5 Å, necessary for observation of NOE interactions. The additional proof for the structure of the $[\text{Ag}(\mathbf{1a})_2]^+$ complex is also provided by the observed trend of the complexation induced shifts in the $c(\text{Ag}^+)/c(\mathbf{1a})$ range of 0.5 and 2.0 (Figure 4, a), where all ligand resonances underwent downfield shifts. This trend could be explained by the disappearance of the $[\text{Ag}(\mathbf{1a})_2]^+$ complex and predominant formation of the $[\text{Ag}(\mathbf{1a})]^+$ complex. The ligand protons close to the metal center [C(4)–H, C(5)–H and C(2')–H] of the 1:1 complex should be more deshielded by Ag^+ coordination through bond effects than those in the 1:2 complex, where these effects are distributed between two bis(oxazoline) units. Indeed, deshielding effects were observed for the C(4)–H and C(5)–H protons on going from a 1:2 to a 1:1 complex. However, the strongest deshielding experienced was of the methyl groups on the bridge, being four bonds away of the Ag^+ coordination site (Figure 4, a). Therefore, the latter effect must come from the shielding of the methyl groups in the 1:2 complex by the π -system of the C(4)-phenyl groups of the second molecule of the ligand $\mathbf{1a}$.

In contrast to $\mathbf{1a}$, the addition of Ag^+ to a CD₃CN solution of $\mathbf{1b}$ produced deshielding of all proton resonances but only slight shielding of the methyl protons; no clear indication of a 1:2 complex could be observed (Figure 4, b). However, processing of the NMR titration data gave the best fit for the formation of $\text{Ag}^+ - \mathbf{1b}$ complexes of 1:2 and 1:1 stoichiometries (see previous paragraph). Comparison of the stability constants determined for $\text{Ag}^+ - \mathbf{1a}$ and $-\mathbf{1b}$ complexes (Table 1) shows that the 1:1 complex of $\mathbf{1b}$ is around seven times more stable than the 1:2 complex, whereas the equivalent complexes of $\mathbf{1a}$ are of approximately the same stability, with the 1:1 complex being margin-

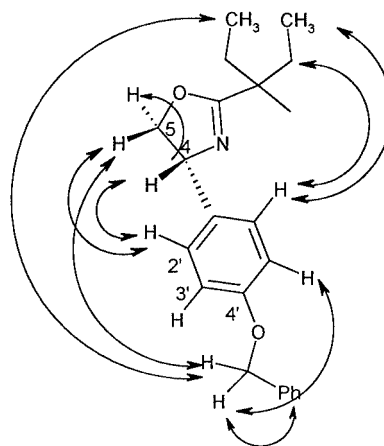


Figure 5. NOE interactions observed in the NOESY spectrum of $[\text{Ag}(\mathbf{1a})_2]^+$

ally more stable. This is reflected in the distribution diagrams of $\text{Ag}^+ - \mathbf{1b}$ and $\text{Ag}^+ - \mathbf{1a}$ systems shown in Figure 6, a, b. At a $c(\text{Ag}^+)/c(\mathbf{1b})$ ratio of 0.5 in the first system the concentration of the 1:1 complex is close to twice that of the 1:2 complex (Figure 6, a). For $\text{Ag}^+ - \mathbf{1a}$ at this concentration ratio, a 1:2 complex is present in approximately four times higher concentration than the 1:1 complex (Figure 6, b). Consequently, the presence of an $\text{Ag}^+ - \mathbf{1a}$ 1:2 complex can be detected through pronounced shielding effects. However, this is not the case for an $\text{Ag}^+ - \mathbf{1b}$ system where the complexation induced shifts are dominated by the prevailing 1:1 complex at low and high $c(\text{Ag}^+)/c(\mathbf{1b})$ ratios. Nevertheless, the observation of shielding effects of methyl groups on the bridge in $\mathbf{1b}$ indicates similar structures of 1:2 $\text{Ag}^+ - \mathbf{1a}$ and $\text{Ag}^+ - \mathbf{1b}$ complexes.

Molecular Modeling

The $[\text{Ag}(\mathbf{1a})_2]^+$ complex was modeled^[48] using 3–5 Å distance constraints between Me and OCH₂Ph protons in accordance with observed NOE interactions. The fully minimized final structure gives N– Ag^+ distances of 1.700, 1.704, 1.704, and 1.710 Å, Me to C(4)–Ph centroid distances of 3.12 Å and Me–OCH₂Ph C–C distances of 3.89 Å, in agreement with observed strong Me shielding and NOEs in the ¹H NMR spectra. The planes containing two bis(oxazoline) units form an angle of 71°, showing pseudotetrahedral coordination (Figure 7, a). The conformational space of the $[\text{Ag}(\mathbf{1a})]^+$ complex was then searched using the systematic search procedure at 30° increments for rotations of 8 rotatable bonds of PhO–CH₂Ph fragments. Five different low-energy conformations with energies within 5 kcal/mol were selected and each was fully minimized (Figure 7, b). The calculated structure reveals high conformational mobility of C(4')–OCH₂Ph fragments and the absence of possible intramolecular aromatic π – π interactions between terminal phenyl groups, is in complete accordance with all experimental results.

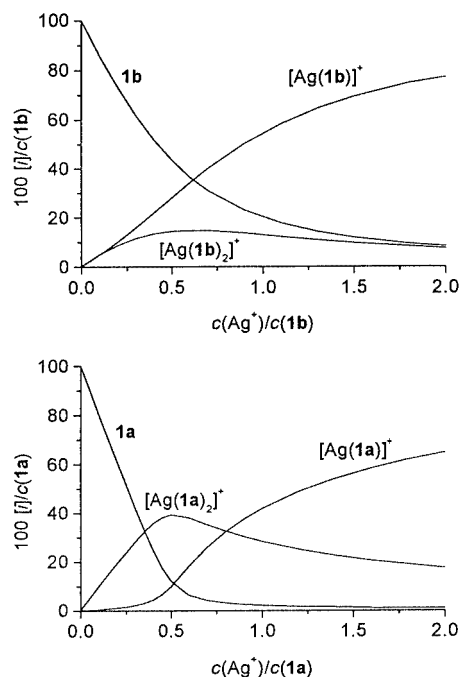


Figure 6. Distribution diagrams of the $\text{Ag}^+/\mathbf{1a}$ and $\text{Ag}^+/\mathbf{1b}$ systems in MeCN; c denotes total concentration, while $[i]$ stands for equilibrium concentration of $i = \text{L}$ ($\mathbf{1a}$ or $\mathbf{1b}$), $[\text{ML}]^+$ and $[\text{ML}_2]^+$ species, respectively

Chiroptical (CD) Study of the Acyclic and Macrocyclic Ligands and Their Copper(I) and Silver(I) Complexes

UV and CD Spectra of Acyclic Bis(oxazolines) **1**

The short-wavelength band ($\lambda_{\text{max}} = 194 \text{ nm}$) can be assigned to the $\pi_{\text{C}=\text{N}}-\pi_{\text{C}=\text{N}}^*$ transition in C_2 -symmetric **1e**, whereas in **1d** it ($\lambda_{\text{max}} = 190 \text{ nm}$) comprises superimposed $^1\text{L}_\text{a}$ bands of the phenyl chromophore. The weak long-wavelength band at $\lambda_{\text{max}} = 264 \text{ nm}$ in the UV spectrum of **1e** is assigned to the conjugated $\pi-\pi^*$ transition, based on the ab initio 6-31G* calculations and analysis of photoelectronic spectra;^[49] **1a** and **1b** show similar UV spectra. However, the spectrum of **1d** is strikingly different showing much less intense bands at 264, 258, and 252 nm corresponding to phenyl substituents. The much more intense band observed at 275 nm for **1a** ($\epsilon = 4700 \text{ M}^{-1}\cdot\text{cm}^{-1}$) as compared to the band at 264 nm for **1d** ($\epsilon = 360 \text{ M}^{-1}\cdot\text{cm}^{-1}$), belongs to the phenoxy group on the stereogenic center.

Absolute configuration of acyclic bis(oxazolines) are (*R,R*) for **1a,c,d** and (*S,S*) for **1b,e**. In the CD spectra of **1a** and **1c** the intense positive band at 205 nm and 204 nm, respectively, is accompanied by a negative band near 192 nm as a sign of exciton interaction between the $^1\text{B}_\text{b}$ transitions. Ligand **1c** with an $\text{O}(\text{CH}_2)_4\text{O}$ bridge between the *para*-phenylene and phenyl rings shows some blue-shift and decreased intensity, presumably due to the increased conformational mobility of the side chains. The third ligand with a phenyl group attached to a stereogenic center (**1d**) shows a ca. 10 times decreased negative band at 190 nm ($\Delta\epsilon < -5 \text{ M}^{-1}\cdot\text{cm}^{-1}$), and a positive band at 198 nm ($\Delta\epsilon = 46.2$

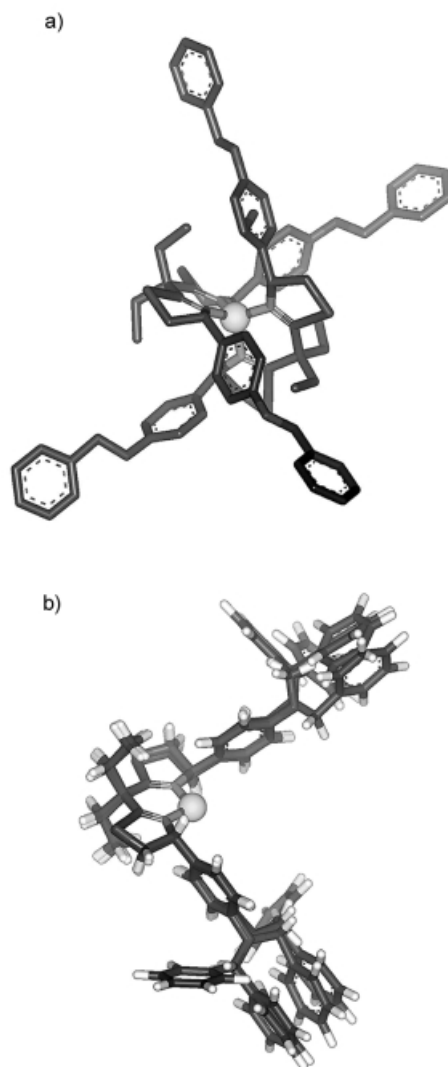


Figure 7. a) Structure of $[\text{Ag}(\mathbf{1a})_2]^+$ generated by molecular modeling; hydrogen atoms are omitted for the sake of clarity; b) five superpositioned low-energy conformations of $[\text{Ag}(\mathbf{1a})]^+$ generated by the systematic search of the conformational space

$\text{M}^{-1}\cdot\text{cm}^{-1}$), only ca 50% less intense than the positive 205-nm band of **1a** and **1c** (Table 2). One can argue that this shift in position and intensity is because of the absence of electron-donating *para*-alkoxy groups in **1d**. In the CD spectra of chiral bis(oxazolines) **1b** and **1e**, having no aromatic substituent at the stereogenic center the bands at 204 and 190 nm, respectively, belong to the $\pi-\pi^*$ transition of the $\text{C}=\text{N}$ chromophore (Table 2). The possibility of a weak exciton interaction between the $^1\text{B}_\text{b}$ transitions of the phenyl chromophores cannot be excluded either.

CD Spectra of Macrocyclic Bis(oxazolines) **2** and **3**

As expected, in the CD spectrum of (*R,R*)-**2a** with oppositely configured chiral centers, as compared to **1b** and **3**, the $^1\text{L}_\text{a}$ band (ca. 230 nm) is positive. However, instead of one, there are two extremely strong bands of opposite sign in the $^1\text{B}_\text{b}$ region of the spectrum. In the UV spectrum a strong absorption was measured at 195 nm that supports the above

Table 2. CD and UV spectroscopic data for acyclic bis(oxazolines) **1a–1e** and their metal complexes in MeCN

Ligand (+ Metal)	Configuration	CD (1st line): λ/nm ($\Delta\epsilon/\text{M}^{-1}\text{ cm}^{-1}$)			
		UV (2nd line): λ/nm ($\epsilon \times 10^{-4}/\text{M}^{-1}\text{ cm}^{-1}$)	$^1\text{B}_b$	$^1\text{L}_a$, $\pi-\pi^*(\text{C}=\text{N})$	$^1\text{L}_b$, $\pi-\pi^*$ or charge transfer
1a	(<i>R,R</i>)	192 (−73.6), 205 (64.22)	229.5(41.2)	277(−0.79)	
		190 (12.1), 196 sh	227 (2.81)	275(0.47)	
1a + Ag^+ , $r_{\text{Ag},1\text{a}} = 1^{[\text{a}]}$		192 (−24.0), 205 (15.0)	226 (12.0), 237 (−2.0)		
1a + Cu^+ , $r_{\text{Cu},1\text{a}} = 1$		196 (20.5), 204.5 (−13.0)	219.5(7.80), 235 (−34.0)	284.5 (0.20)	
1b	(<i>S,S</i>)	204 (−16.8)	$\approx 229\text{sh}$	282 (0.31)	
		190.5 (12.7), 195.5 sh	225.5(2.7)	275.5 (0.51)	
1b + Ag^+ , $r_{\text{Ag},1\text{b}} = 1^{[\text{a}]}$		196.5 (1.02)	206 (−4.05), 237 (−1.78)		
1b + Cu^+ , $r_{\text{Cu},1\text{b}} = 1$		198 (−7.23)	207 (−4.23), 229.5 (5.83)	281 (−0.69)	
1c	(<i>R,R</i>)	190.5 (−58.2), 204 (64.7)	229 (37.6)	277 (−0.94)	
		195(11.7)	224.5 (2.75)		
1c + Cu^+ , $r_{\text{Cu},1\text{c}} = 1$		196 (7.50), 202.5 (−6.98)	213sh 221(10.8) 235(−23.2)	285 (0.095)	
1d	(<i>R,R</i>)	< 190 (< −5), 198 (46.2)	214 (31.9)	256 (0.50)	
		< 190 (> 12)	207 (3.17)	252 (0.043), 258 (0.048), 264 (0.036)	
1e	(<i>S,S</i>)	190 (−10.0)	229 sh (−3.13)	^[b]	
		194 (0.88)	222 sh (0.09)	264 (very weak)	

^[a] Continuous spectral changes up to $r_{\text{Ag},\text{L}} \approx 5$. ^[b] No band could be measured even with a 1-cm cell.

assignment. Clearly, the strong bands at 204 and 194 nm are due to the *para*-substituted phenyl chromophores attached to the stereogenic centers (Table 3). Notably, a couplet in the $^1\text{B}_b$ band spectral region was observed for **1a** with *para*-alkoxyphenyl substituents but not for **1b** with *para*-alkoxybenzyl groups.

Regardless of the length of the alkyl chain ($n = 2-5$), the macrocyclic ligands **2a–d** with *para*-alkoxy-substituted phenyl groups attached to the stereogenic centers show CD spectra marked by an almost symmetric exciton couplet in the $^1\text{B}_b$ region. The most intense bands turn up in the spectrum of (*R,R*)-**2b** ($n = 3$) [204 nm ($90.5 \text{ M}^{-1}\text{cm}^{-1}$) and 193 nm ($-73.0 \text{ M}^{-1}\text{cm}^{-1}$), respectively]. The positive sign of the couplet is compatible with the orientation of the $^1\text{B}_b$ electric transition moment vectors, as discussed in the final section. On the basis of the increased intensity of the $^1\text{L}_a$ bands, a weaker exciton interaction between the $^1\text{L}_a$ transitions cannot be excluded either. However, instead of the expected negative band near 220 nm, the spectra of all mac-

rocycles of type **2** have a positive CD (mostly two positive shoulders) between 225 and 205 nm. The lack of an exciton couplet in the $^1\text{L}_a$ region can be attributed to the nearly parallel orientation of the electric transition vector (Table 3). A positive band appears in the spectrum of **2b** at 220 nm. The complexity of the spectrum clearly indicates that the CD contribution of the “lower half” of the molecule cannot be completely neglected. Because of the increased flexibility, this part of the molecule likely occurs as a mixture of conformers but the dominant one(s) are expected to have the same sign of helical twist of the *para*-alkoxyphenyl rings attached to the $\text{C}(\text{Et})_2$ bridge.

The CD spectrum of (*S,S*)-**3** is dominated by two negative bands at 203.5 and 228 nm which can be assigned to the $^1\text{B}_b$ and $^1\text{L}_a$ band, respectively, of the *para*-alkoxybenzyl chromophores attached to stereogenic centers. A weak positive and some weaker negative bands are seen in the $^1\text{L}_b$ region of the spectrum (Table 3). In the spectrum of the related acyclic analog (*S,S*)-**1b** ($\text{R} = \text{Bzl}-\text{O}-\text{Bzl}$) the cor-

Table 3. CD and UV spectroscopic data for macrocyclic bis(oxazolines) **2a–2d** and **3** and their metal complexes in MeCN

Ligand (+ metal)	CD (1st line): λ/nm ($\Delta\epsilon/\text{M}^{-1}\text{ cm}^{-1}$) UV (2nd line): λ/nm ($\epsilon \times 10^{-4}/\text{M}^{-1}\text{ cm}^{-1}$)	$^1\text{B}_b$	$^1\text{L}_a$, $\pi-\pi^*(\text{C}=\text{N})$	$^1\text{L}_b$
(<i>R,R</i>)- 2a	194 (−71.0), 204 (83.9) 195 (12.6)	\approx 211 sh, \approx 218 sh, 233 (37.0) 226 (3.18)	283 (−0.61) 276 (0.61)	
(<i>R,R</i>)- 2b	193 (−73.00), 204 (90.5) 195 (12.9)	220 (25.8), 232 (37.8) 226 (3.27)	284.5 (−0.62) 276 (0.73)	
(<i>R,R</i>)- 2c	191.5 (−65.5), 204 (75.2) 196 (13.5)	\approx 212 sh, 231 (38.2) 227 (3.40)	277 (−0.83), 290–325 (weak positive bands) 276 (0.77)	
(<i>R,R</i>)- 2d	191.5 (−66.6), 203.5 (81.2) 196 (13.8)	\approx 211 sh, \approx 222 sh 232 (37.0) 227 (3.69)	276 (−1.07) 276.5 (0.83)	
(<i>S,S</i>)- 3	203.5 (−19.8) 194.5 (15.3)	228 (−6.40) 226 (3.66)	277 (−0.072), 282.5 (0.07), 299.5 (−0.05)	
+ Ag^+ , $r_{\text{Ag},3} = 1^{[\text{a}]}$	203.5 (−14.9)	229 (−6.50)	273.5 sh (−0.29) weak positive bands above 300 nm	
+ Cu^+ , $r_{\text{Cu},3} = 1$	209 (−6.80)	\approx 222 sh	261 (0.68), 287 sh, 311.5 (−0.145)	

^[a] Continuous spectral changes up to $r_{\text{Ag},3} \approx 4$.

responding bands turn up at 204 nm ($-16.8 \text{ M}^{-1}\text{cm}^{-1}$), 229 nm (sh) and 282 nm. The lack of exciton splitting in the far-UV spectral region of **1b** and **3** is attributed to the difference in geometry and the greater conformational freedom of the *para*-alkoxybenzyl chromophores.

CD Spectra of Copper(I) and Silver(I) Complexes

In order to study their complexation by CD, acyclic ligands **1a–c** as well as the corresponding macrocyclic analogs **2a–d** and **3** were titrated with Ag^+ and Cu^+ ions.

In the spectrum of the acyclic ligand **1a** the exciton couplet of the $^1\text{B}_b$ transition was destroyed by Cu^+ complexing. A strong negative and a weaker positive band replaced the positive $^1\text{L}_a$ band at 229.5 nm (Figure 8). The spectrum showed only small changes between $r_{\text{Cu},1a} = 1$ and 2 [$r_{\text{M,L}} = c(\text{M})/c(\text{L})$] that suggests formation of a 1:1 complex of significant stability, in accordance with the results of the UV titration. Titration of **1a** with Ag^+ ions gave rise to a gradual decrease of the band intensities of the couplet. Significant spectral changes were observed also in the $^1\text{L}_a$ band region: a relatively strong negative band appeared at $r_{\text{Ag},1a} \geq 1$, while position and intensity of the band at 205 nm in the spectrum of **1a** varied gradually up to $r_{\text{Ag},1a} = 5$ (Figure 9). This spectral behavior can be explained by the formation of a 1:1 complex of lower stability compared to $[\text{Cu}(\mathbf{1a})]^+$. Ligand **1c** showed a similar spectral response to Ag^+ as **1a**. Cu^+ broke the positive couplet at $r_{\text{Cu},1c} \geq 0.75$ and the titration data indicated formation of a stable 1:1 Cu^+ complex.

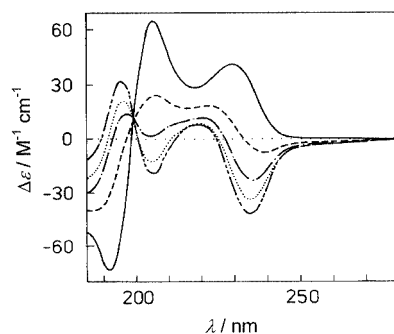


Figure 8. CD spectra of free (*R,R*)-**1a** (—), and on addition of Cu^+ ; 1:0.5 (---), 1:0.75 (— · —), 1:1 (····), and 1:2 (----)

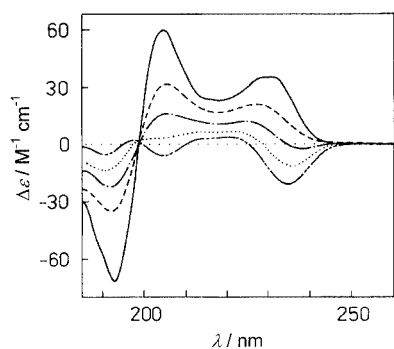


Figure 9. CD spectra of free (*R,R*)-**1a** (—), and on addition of Ag^+ ; 1:0.5 (---), 1:1 (— · —), 1:2 (····), and 1:5 (----)

Titration of **1b** with Ag^+ resulted in gradual spectral changes up to $r_{\text{Ag},1b} = 5$ (Figure 10). The formation of a 1:1 complex of exceeding stability could not be detected (Table 2). No definite spectral changes were seen between $r_{\text{Ag},1b} = 5$ and 10. Addition of Cu^+ caused marked spectral changes in the $^1\text{L}_a$ band region. Above $r_{\text{Cu},1b} = 1$ the main feature of the spectra is a positive band at ca. 230 nm. The formation of no dominant 1:1 complex could be detected (Figure 11).

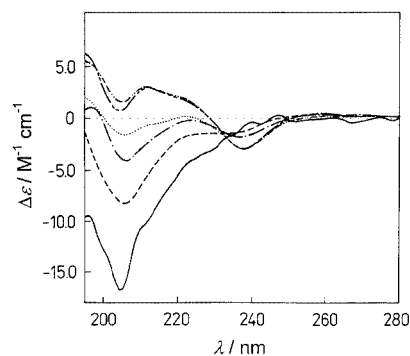


Figure 10. CD spectra of free (*S,S*)-**1b** (—), and on addition of Ag^+ ; 1:0.5 (---), 1:1 (— · —), 1:2 (····), 1:5 (----), and 1:10 (— · · · —)

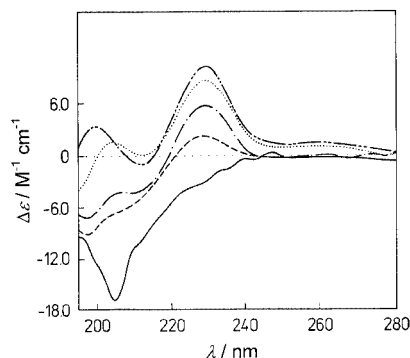


Figure 11. CD spectra of free (*S,S*)-**1b** (—), and on addition of Cu^+ ; 1:0.5 (---), 1:1 (— · —), 1:2 (····), and 1:5 (----)

Macrocyclic ligands **2a–d** showed a similar behavior against Ag^+ . The couplet was completely destroyed at an $r_{\text{Ag},2} \geq 2$ ratio in the case of $n = 2$ and 5 (Figure 12); Cu^+ proved to be a more efficient breaker of the couplet. The spectra reflected no exciton interaction at $r_{\text{Cu},2} \geq 1$ for ligands **2**, $n = 2$ and 4. At $r_{\text{Cu},2} > 1$ the $^1\text{L}_a$ band appeared as a pair of negative and positive bands. The $^1\text{B}_b$ couplet, characteristic for the spectra of ligands **2a–d**, was replaced by a shoulder at ca. 210 nm and a pair of weaker blue-shifted oppositely signed bands (Figure 13) at $r_{\text{Cu},2} > 1$. Increasing the amount of Cu^+ gave rise to further spectral shifts, both below and above 250 nm. This spectral behavior can be interpreted as the consequence of the formation of a 1:1 complex of lower stability. However, the occurrence of complexes of other stoichiometry cannot be excluded either.

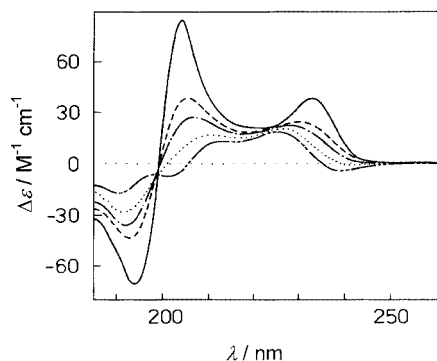


Figure 12. CD spectra of free (*R,R*)-**2a** (—), and on addition of Ag^+ ; 1:0.5 (---), 1:1 (— · —), 1:2 (····), and 1:5 (----)

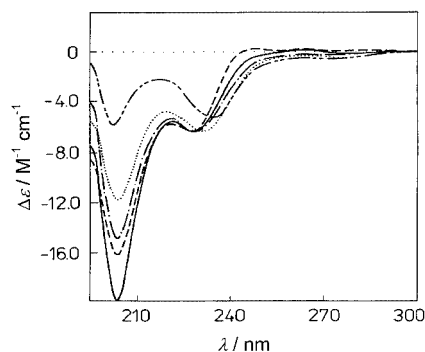


Figure 14. CD spectra of free (*S,S*)-**3** (—), and on addition of Ag^+ ; 1:0.5 (---), 1:1 (— · —), 1:2 (····), and 1:7.8 (----)

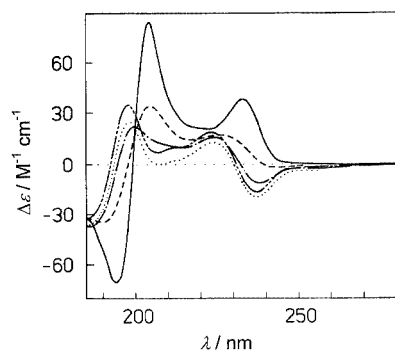


Figure 13. CD spectra of free (*R,R*)-**2a** (—), and on addition of Cu^+ ; 1:0.5 (---), 1:1 (— · —), 1:2 (····), and 1:5 (----)

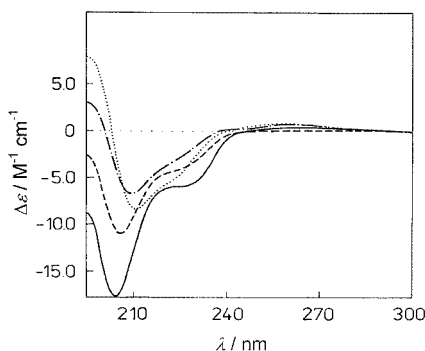


Figure 15. CD spectra of free (*S,S*)-**3** (—), and on addition of Cu^+ ; 1:0.5 (---), 1:1 (— · —), and 1:2 (····)

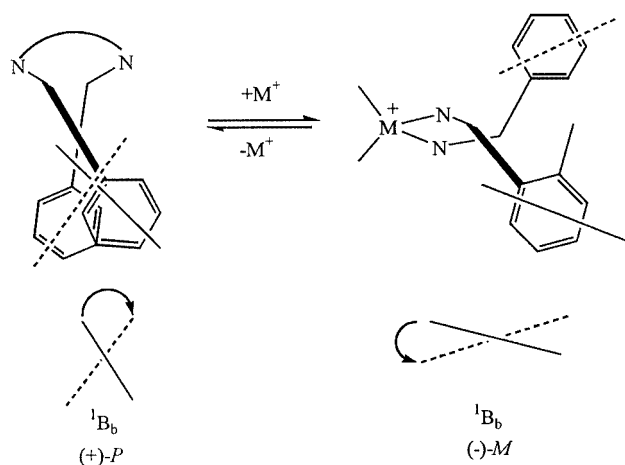
Addition of Ag^+ to the macrocyclic ligand **3** resulted in an almost continuous spectral change (Figure 14). The position and intensity of the $^1\text{L}_a$ band at 228 nm were less influenced than that of the more intense $^1\text{B}_b$ band at 203.5 nm. Interestingly, the weak negative band at 299.5 nm of **3** with vibrational fine structure changed only to a small extent, while the weak positive band at 282.5 nm of **3** was blue-shifted, changed sign and appeared with increased intensity upon addition of Ag^+ (Table 3). Accordingly, the latter band can be assigned to the $n-\pi^*$ transition of the $\text{C}=\text{N}$ groups, the nitrogen atoms of which coordinate to a central cation. Addition of Cu^+ to **3** changed the spectrum continuously up to a 2:1 metal/ligand molar ratio ($r_{\text{Cu},3} = 2$) (Figure 15). Complexing of Cu^+ by **3** gave rise to an increase in the intensity of both long-wavelength bands. The negative band showed a red-shift while the positive one a more definite (> 20 nm) blue-shift (Table 3). The weak negative band at ca. 310 nm of the 1:1 Cu^+ complex likely belongs to the complexed Cu^+ ion. In the far-UV region, both bands showed definite intensity and wavelength shifts up to $r_{\text{Cu},3} = 2$.

Conformations of Free Ligand **1a** and Its Copper(I) and Silver(I) Complexes in Solution

There are few reports on comparative spectroscopic study of (poly)nitrogen ligands and their metal complexes. In an early study Bosnich has observed the split of $\pi-\pi^*$ transitions and the nearly equal positive and negative CD bands (couplet) for Zn^{2+} complexes with 1,4-*N,N*-bidentate ligands derived from salicylaldehyde (salene), comprising strong conjugated chromophores, and the presence of exciton interaction was demonstrated.^[50,51] *transoid* conformation of the free ligand was observed in solution of 6,6'-disubstituted 2,2-bipyridine,^[52,53] and its rotation into a *cisoid* conformer on complexation with Co^{2+} , affording a complex of C_2 symmetry, is documented by X-ray analysis of the complex.^[54] Williams et al. have recently reported on the enantiopure helicates, complexes of chiral 2,6-bis(oxazolyl)pyridines as tridentate nitrogen ligands and an Ag^+ ion.^[44,45] They had observed large changes in the CD spectrum of the ligand upon complex formation. The free ligand shows a weak negative band in the UV region of the spectrum ($\Delta\epsilon_{296} = -0.4 \text{ M}^{-1}\cdot\text{cm}^{-1}$), whereas the complex shows a strong positive band ($\Delta\epsilon_{301} = 10.15 \text{ M}^{-1}\cdot\text{cm}^{-1}$, for one metal center), corresponding to a new shoulder in the UV/Vis spectrum ($\epsilon = 1547 \text{ M}^{-1}\cdot\text{cm}^{-1}$). This CD activity was attributed to a fixed helical conformation of the ligand in the complex, whereas free ligands may adopt different con-

formations that cancel out each other in the CD spectrum. Similar phenomena have been observed for several ligands^[55–57] and metal complexes,^{[44][58][59]} and explained by the exciton theory.

For the free bis(oxazoline)-type ligands, the conformation in solution is not known. We have therefore performed MM calculations^[48] for an analog of **1a** (for better visualization methyl substituents are attached instead of benzyl), and the most stable conformation found was the helically twisted *transoid* one. In this conformation two phenyl groups form a positive (*P*) twist, and therefore a positive CE for the 1B_b band is expected, (Scheme 1, Figure 16). In the 1:1 complex $Cu^+ - \mathbf{1a}$ two halves of bis(oxazoline) are fixed in the nearly coplanar *cis* position with two large groups on the stereogenic centers forming a “picket-fence” topology, important for high enantioselectivity in catalytic reactions.^[60]



Scheme 1. Schematic presentation of interacting chromophores in **1a** and **1a**–metal complex, and position of their 1B_b transition vectors in the free ligand and in the complex

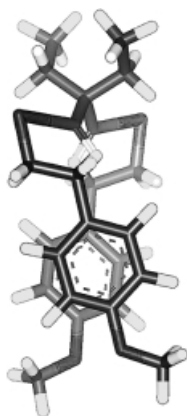


Figure 16. Ball-and-stick model of the non-hydrogen atoms of an analog of **1a** based on MM2 calculations

It is interesting that no such straight-forward change of the CD of **1a** is observed on titration with Ag^+ ions (Figure 9). The inflection point at ca. 195 nm is maintained, revealing formation of an $[Ag(\mathbf{1a})_2]^+$ complex, as confirmed

by the NMR titration, but only partial inversion of the sign of the two bands of the couplet is observed. This reveals different influence of Cu^+ and Ag^+ on conformational change of **1a** upon complexation.

Generally, diminished intensity of the short-wavelength band on complexation of **1a** and **1b** is presumably raised by depleting π - and n -electron density in the $C=N$ group on coordination to the metal ion. Since any stronger exciton coupling between two $C=N$ chromophores, which are non-planar in the free ligand, seems to be absent, coplanarization of the 4π system on complexation should result in an enhanced intramolecular charge transfer, and consequently could influence only the long-wavelength transition band at ca 280 nm.

Conclusion

Combined achiral and chiral spectroscopic study of 1,5-dinitrogen ligands with C_2 -symmetric **1a** and **1b** and their copper(I) and silver(I) complexes has shown that they form stable 1:2 metal/ligand complexes, which transform on ulterior addition of metal ions to 1:1 complexes. Modeling experiments indicate pseudotetrahedral arrangement of coordinating N atoms around the central metal ion in the $[Ag(\mathbf{1a})_2]^+$ complex. The stability constants (Table 1) were determined for $Cu^+ -$ and $Ag^+ - \mathbf{1a}$ and $-\mathbf{1b}$ complexes of 1:2 and 1:1 stoichiometries. At low cation/ligand molar ratios, 1:2 complexes are formed with Cu^+ . The stabilities of 1:1 complexes exceed those of 1:2 complexes for one order of magnitude. The catalytic 1:1 Cu^+ complexes of **1a** and **1b** used in stereoselective cyclopropanations have stability constants of ca. $10^5 M^{-1}$ in acetonitrile. A 1H NMR study of the **1a**– Ag^+ complexation reveals the formation of an $[Ag(\mathbf{1a})_2]^+$ complex with a stability constant of ca. $10^3 M^{-1}$. The observed complexation induced shifts and NOEs together with molecular modeling suggest formation of a pseudotetrahedral complex. The comparative CD study of free acyclic (**1a–e**) and macrocyclic (**2a–d**, **3**) ligands and their Cu^+ and Ag^+ complexes provided insight into conformational changes occurring upon formation of the complexes. For free ligands **1a**, **1c** and **2a–d** strong exciton coupling in the 1B_b region was observed and explained by a positive helicity of the alkoxyphenyl substituents on the stereogenic centers. Addition of a Cu^+ ion destroys the couplet and leads to opposite CE. The latter is the consequence of the ligand conformational change from *transoid* in the free ligand to *cisoid* in the Cu^+ complex and formation of a negative helicity between two alkoxyphenyl substituents. Such spectral properties are not observed for **1b** and **3** possessing more flexible benzyl substituents at the stereogenic centers.

Experimental Section

General: Compounds **1d** and **1e** are commercially available. Preparation of the compounds **2a–d** is reported in ref.^[31] and the pre-

paration of the compounds **1a–c** and **3** will be published elsewhere. Reagents were purchased from Aldrich or Fluka and were used without further purification. All solvents were purified and dried according to standard procedures.

Spectrometric Titrations: UV titrations were performed at $(25 \pm 0.1)^\circ\text{C}$ by means of a Varian Cary 5 spectrophotometer equipped with a thermostating device. The spectral changes of **1a** and **1b** solutions ($c = 5 \cdot 10^{-5} \text{ mol} \cdot \text{dm}^{-3}$) in MeCN were recorded upon stepwise addition of copper(I) ions directly into the measuring quartz cell (1 cm). Copper(I) ions were added as $[(\text{CH}_3\text{CN})_4\text{Cu}]\text{PF}_6$ solution ($c = 2.6 \cdot 10^{-4} \text{ mol} \cdot \text{dm}^{-3}$) in MeCN. Spectra were sampled at 1-nm intervals. Fluorimetric titrations ($\lambda_{\text{exc}} = 277 \text{ nm}$, $\lambda_{\text{em}} = 285\text{--}330 \text{ nm}$, filter = 290 nm) were carried out using a Perkin–Elmer LS-50 spectrofluorimeter at ambient temperature. The MeCN solutions of **1a** and **1b** ($c = 1.32 \cdot 10^{-5} \text{ mol} \cdot \text{dm}^{-3}$) were placed in the measuring quartz cell (1 cm) and titrated with an MeCN solution of AgBF_4 ($c = 0.0116 \text{ mol} \cdot \text{dm}^{-3}$ and $0.116 \text{ mol} \cdot \text{dm}^{-3}$). ^1H NMR titrations of **1a** and **1b** were performed at ambient temperature in CD_3CN (data taken as $\Delta\delta/\text{ppm}$ according to the signal of solvent used as internal standard) with Varian Gemini 300 MHz [$c(\mathbf{1a}) = 0.02 \text{ mol} \cdot \text{dm}^{-3}$, $V_0 = 0.5 \text{ mL}$, $c(\text{AgBF}_4) = 0.1 \text{ mol} \cdot \text{dm}^{-3}$] and a Bruker 500 MHz instruments [$c(\mathbf{1b}) = 0.001 \text{ mol} \cdot \text{dm}^{-3}$, $V_0 = 0.5 \text{ mL}$, $c(\text{AgBF}_4) = 0.005 \text{ mol} \cdot \text{dm}^{-3}$]. Aliquots of the metal ion solution were added into the solution of the ligand in an NMR probe with Hamilton syringes. The obtained spectrometric data were processed using the SPECFIT program.^[47] CD titrations: UV/Vis and CD spectra were recorded in acetonitrile with a Jobin–Yvon VI dichrograph calibrated with epiandrosterone. The ligands were titrated with AgBF_4 and $[(\text{CH}_3\text{CN})_4\text{Cu}]\text{PF}_6$, respectively, in both the long-wavelength ($> 240 \text{ nm}$) and short-wavelength UV regions. Measurements were performed at room temperature in 0.02- and 0.1-cm cells. The spectral changes of ligand solutions ($c = 4.5\text{--}6.0 \cdot 10^{-4} \text{ mol} \cdot \text{dm}^{-3}$) in MeCN were recorded upon addition of silver(I) ($c = 2.0 \cdot 10^{-2} \text{ mol} \cdot \text{dm}^{-3}$) and copper(I) ($c = 8.0 \cdot 10^{-3} \text{ mol} \cdot \text{dm}^{-3}$) solutions in MeCN, respectively.

Molecular Modeling: The metal-free bis(oxazoline) ligand was docked on the complex $\text{Ag}^+/\mathbf{1d}$ and the low-energy structure obtained modified by adding two additional N–heavy atom bonds to obtain the tetracoordinated complex. The metal–N bonds of 2.18 Å were used as distance constraints and the complex was fully minimized. In the next step, a benzyloxy group was attached in the *para* position to the stereogenic center of each phenyl ring to generate the 1:2 $\text{Ag}^+/\mathbf{1a}$ complex. The molecular modeling of the 1:2 $\text{Ag}^+/\mathbf{1a}$ complex and the search of the conformational space of the 1:1 $\text{Ag}^+/\mathbf{1a}$ complex was performed using the SYBYL molecular modeling software, version 6.3 of TRIPOS Inc. 4,4'-Diphenylbis(oxazoline) complex $\mathbf{1d}\text{--Ag}^+$ was constructed using the Builder module. Instead of the Ag^+ ion, a heavy atom parameter available in the SYBYL package was used together with N–heavy atom distance constraints of 2.18 Å corresponding to an N– Ag^+ bond length found in the X-ray structure of some tetracoordinated Ag^+ –bis(oxazoline) helicates.^[44] The Gasteiger–Hückel charges were used with +1 formal charge of the heavy atom and the complex was minimized.

Acknowledgments

The financial support from the Croatian Ministry of Science and Technology (Program 009807) and the Hungarian Scientific Research Fund (OTKA Nr.T034866) is gratefully acknowledged.

- [1] *Comprehensive Asymmetric Catalysis* (Eds.: E. N. Jacobsen, A. Pfaltz, H. Yamamoto), Springer, Berlin, Heidelberg, 1999.
- [2] R. Noyori, *Asymmetric Catalysis in Organic Synthesis*, J. Wiley & Sons, New York, 1993.
- [3] F. Fache, E. Schulz, M. L. Tommasino, M. Lemaire, *Chem. Rev.* **2000**, *100*, 2159–2231.
- [4] A. K. Ghosh, P. Mathivanan, J. Cappiello, *Tetrahedron: Asymmetry* **1998**, *9*, 1–45.
- [5] A. Pfaltz, *Acta Chem. Scand.* **1996**, *50*, 189–194.
- [6] R. E. Lowenthal, A. Abiko, S. Masamune, *Tetrahedron Lett.* **1990**, *31*, 6005–6008.
- [7] R. E. Lowenthal, S. Masamune, *Tetrahedron Lett.* **1991**, *32*, 7373–7376.
- [8] D. A. Evans, K. A. Woerpel, M. M. Hinman, M. M. Faul, *J. Am. Chem. Soc.* **1991**, *113*, 726–728.
- [9] D. A. Evans, K. A. Woerpel, M. J. Scott, *Angew. Chem. Int. Ed. Engl.* **1992**, *31*, 430–432.
- [10] C. Pique, B. Fahndrich, A. Pfaltz, *Synlett* **1995**, 491–492.
- [11] O. Hoarau, H. Ait-Haddou, M. Castro, G. G. A. Balavoine, *Tetrahedron: Asymmetry* **1997**, *8*, 3755–3764.
- [12] D. A. Evans, M. M. Faul, M. T. Bilodeau, B. A. Anderson, D. M. Barnes, *J. Am. Chem. Soc.* **1993**, *115*, 5328–5329.
- [13] K. B. Hansen, N. S. Finney, E. N. Jacobsen, *Angew. Chem. Int. Ed. Engl.* **1995**, *34*, 676–678.
- [14] A. S. Gokhale, A. B. E. Minidis, A. Pfaltz, *Tetrahedron Lett.* **1995**, *36*, 1831–1834.
- [15] D. A. Evans, S. J. Miller, T. Lectka, *J. Am. Chem. Soc.* **1993**, *115*, 6460–6461.
- [16] D. A. Evans, D. M. Barnes, *Tetrahedron Lett.* **1997**, *38*, 57–58.
- [17] D. A. Evans, E. A. Shaughnessy, D. M. Barnes, *Tetrahedron Lett.* **1997**, *38*, 3193–3196.
- [18] D. A. Evans, J. S. Johnson, *J. Org. Chem.* **1997**, *62*, 786–787.
- [19] D. A. Evans, J. S. Johnson, C. S. Burgey, K. R. Campos, *Tetrahedron Lett.* **1999**, *40*, 2879–2882.
- [20] D. A. Evans, J. A. Murry, M. C. Kozlowski, *J. Am. Chem. Soc.* **1996**, *118*, 5814–5815.
- [21] A. Bernardi, G. Colombo, C. Scolastico, *Tetrahedron Lett.* **1996**, *37*, 8921–8924.
- [22] D. A. Evans, T. Rovis, M. C. Kozlowski, J. S. Tedrow, *J. Am. Chem. Soc.* **1999**, *121*, 1994–1995.
- [23] N. Gathergood, W. Zhaang, K. A. Jorgensen, *J. Am. Chem. Soc.* **2000**, *122*, 12517–12522.
- [24] A. E. Russell, S. P. Miller, J. P. Morken, *J. Org. Chem.* **2000**, *65*, 8381–8383.
- [25] D. Mueller, G. Umbricht, B. Weber, A. Pfaltz, *Helv. Chim. Acta* **1991**, *74*, 232–240.
- [26] P. von Matt, G. C. Lloyd-Jones, A. B. E. Minidis, A. Pfaltz, L. Macko, M. Neuburger, M. Zehnder, H. Ruegger, P. S. Pregosin, *Helv. Chim. Acta* **1995**, *78*, 265–284.
- [27] O. Hoarau, H. Ait-Haddou, J.-C. Daran, D. Cramailere, G. G. A. Balavoine, *Organometallics* **1999**, *18*, 4718–4723.
- [28] J. Wu, R. Radinov, N. A. Porter, *J. Am. Chem. Soc.* **1995**, *117*, 11029–11030.
- [29] M. Nakamura, M. Arai, E. Nakamura, *J. Am. Chem. Soc.* **1995**, *117*, 1179–1180.
- [30] S. Hanessian, R.-Y. Yang, *Tetrahedron Lett.* **1996**, *37*, 8997–9000.
- [31] T. Portada, M. Roje, Z. Raza, V. Čaplar, M. Žinić, V. Šunjić, *Chem. Commun.* **2000**, 1993–1994.
- [32] Z. Raza, S. Đaković, V. Vinković, V. Šunjić, *Croat. Chem. Acta* **1996**, *69*, 1545–1559.
- [33] S. Đaković, L. Liščić-Tumir, S. I. Kirin, V. Vinković, Z. Raza, A. Šuste, V. Šunjić, *J. Mol. Catal. A* **1997**, *118*, 27–31.
- [34] V. Šunjić, D. Šepac, B. Kojić-Prodić, R. Kiralj, K. Mlinarić-Majerski, V. Vinković, *Tetrahedron: Asymmetry* **1993**, *4*, 575–590.
- [35] S. I. Kirin, V. Vinković, V. Šunjić, *Chirality* **1995**, *7*, 115–120.
- [36] Zs. Majer, M. Hollosi, S. I. Kirin, V. Šunjić, *Chirality* **1996**, *8*, 244–248.
- [37] M. Onishi, K. Isagawa, *Inorg. Chim. Acta* **1991**, *179*, 155–156.

- [38] C. Bolm, K. Weickhardt, M. Zehnder, T. Rauff, *Chem. Ber.* **1991**, *124*, 1173–1180.
- [39] J. Hall, J.-M. Lehn, A. DeCian, J. Fischer, *Helv. Chim. Acta* **1991**, *74*, 1–6.
- [40] H. Nishiyama, K. Aoki, H. Itoh, T. Iwamura, N. Sakata, O. Kurihara, Y. Motoyama, *Chem. Lett.* **1996**, 1071–1072.
- [41] S. Kanemasa, Y. Oderaotoshi, H. Yamamoto, J. Tanaka, E. Wada, D. P. Curran, *J. Org. Chem.* **1997**, *62*, 6454–6455.
- [42] R. P. Singh, *Synth. React. Inorg. Met.-Org. Chem.* **1997**, *27*, 155–166.
- [43] C. J. Fahrni, A. Pfaltz, M. Neuburger, M. Zehnder, *Helv. Chim. Acta* **1998**, *81*, 507–524.
- [44] C. Provent, S. Hewage, G. Brand, G. Bernardinelli, L. J. Charbonniere, A. F. Williams, *Angew. Chem. Int. Ed. Engl.* **1997**, *36*, 1287–1289.
- [45] C. Provent, E. Rivara-Minten, S. Hewage, G. Brunner, A. F. Williams, *Chem. Eur. J.* **1999**, *5*, 3487–3494.
- [46] J. Balsells, J. M. Betancort, P. J. Walsh, *Angew. Chem. Int. Ed.* **2000**, *39*, 3428–3430.
- [47] R. A. Binstead, A. D. Zuberbühler, *SPECFIT Program, Global Least-Squares Fitting by Factor Analysis and Marquart Minimization*, Spectrum Software Associates, Chapel Hill, NC, **1994**.
- [48] SYBYL, *Molecular Modeling Software*, version 6.3, TRIPOS Inc.
- [49] B. Kovač, L. Klasinc, Z. Raza, V. Šunjić, *J. Chem. Soc., Perkin. Trans. 2* **1999**, 2455–2459.
- [50] S. F. Mason, *Quart. Rev.* **1963**, *17*, 20–66.
- [51] B. Bosnich, *J. Am. Chem. Soc.* **1968**, *90*, 627–632.
- [52] A. Castelano, H. Guenther, S. Ebensole, *J. Phys. Chem.* **1965**, *12*, 4166–4176.
- [53] T. McL. Spotswood, C. I. Tanzer, *Aust. J. Chem.* **1967**, *20*, 1227–1242.
- [54] C. Bolm, “Optically Active Bipyridines in Enantioselective Catalysis” in: *Organic Synthesis via Organometallics* (Eds.: K. H. Doetz, R. W. Hoffmann), Vieweg, Braunschweig, **1991**, pp. 223–240.
- [55] N. C. Fletcher, F. R. Keene, M. Ziegler, H. Stoeckli-Evans, H. Viebrock, A. von Zelewsky, *Helv. Chim. Acta* **1996**, *79*, 1192–1202.
- [56] N. Harada, K. Nakanishi, *Circular Dichroic Spectroscopy. Exciton Coupling in Organic Chemistry*, University Science Books, Mill Valley, CA, **1983**.
- [57] V. Buss, S. Falzewski, K. Kolster, *J. Org. Chem.* **1999**, *64*, 1071–1073.
- [58] O. Mamula, A. von Zelewsky, G. Bernardinelli, *Angew. Chem. Int. Ed.* **1998**, *37*, 290–293.
- [59] O. Mamula, A. von Zelewsky, T. Bark, H. Stoeckli-Evans, A. Neels, G. Bernardinelli, *Chem. Eur. J.* **2000**, *6*, 3575–3585.
- [60] M. P. Doyle, “Asymmetric Cyclopropanation”, in: *Catalytic Asymmetric Synthesis* (Ed.: I. Ojima), VCH, **1993**, pp. 63–99.

Received January 8, 2002
[102008]